COMPUTER AIDED DIAGNOSIS SYSTEM IN DIGITAL MAMMOGRAPHY

João Maria Patacho de Matos Rocha e Melo

Discussion of the Thesis to obtain the Master of Science Degree in

Electrical and Computer Engineering

Supervisors: Prof. Maria Margarida Campos da Silveira
Prof. Nuno Miguel de Pinto Lobo e Matela

Examination Committee

Chairperson: Prof. João Fernando Cardoso Silva Sequeira
Supervisor: Prof. Maria Margarida Campos da Silveira
Members of the Committee: Prof. Jorge dos Santos Salvador Marques

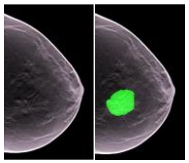

OUTLINE

- Context and Motivation
- Pre-processing and Segmentation
- Feature Extraction and Classification
- Experimental Results
- Conclusions and Future Work

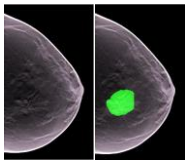

1.1 CANCER STATISTICS

- 14.1 million cases of cancer in 2012
- Breast cancer represents 25% of all cancer cases among the female population
- High survival rates if caught in early stages

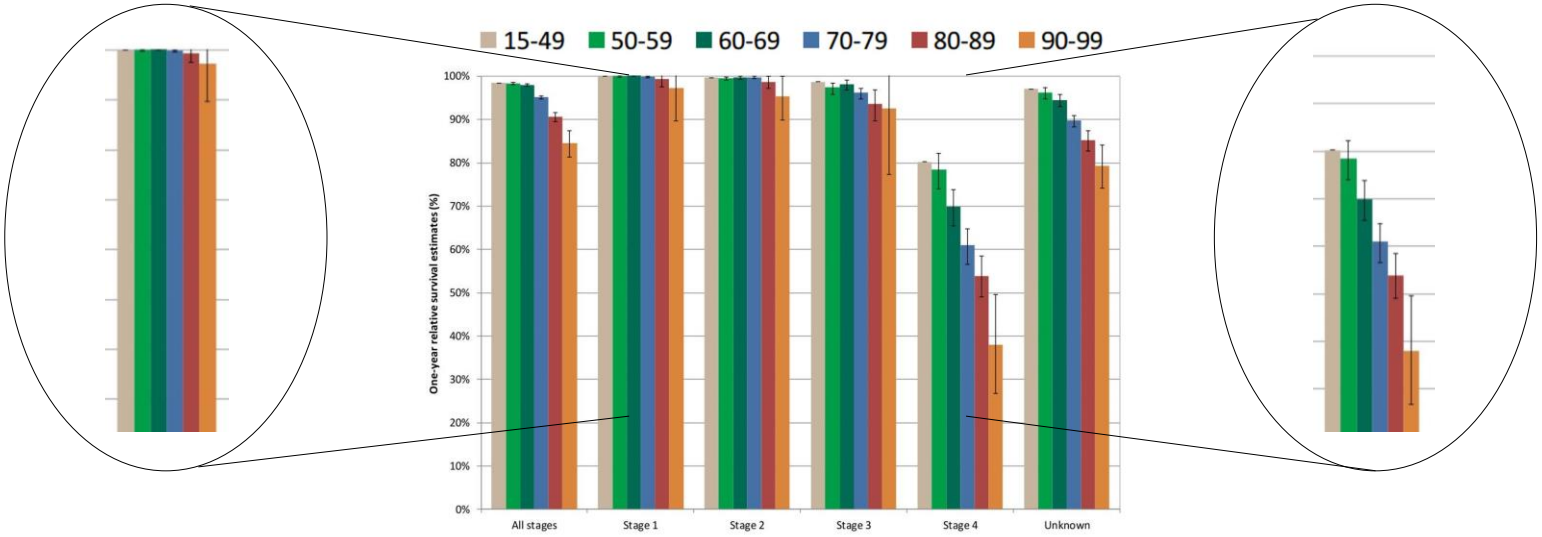

Figure 1 – Survival rate broke down by stage and age sector

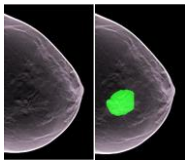

1.3 BREAST IMAGING TECHNIQUES

MAMMOGRAPHY

- Most common breast imaging technique
- X-Ray based
- Standard Views:
  - Craniocaudal (Fig 2)
  - MedioLateral Oblique (Fig 3)

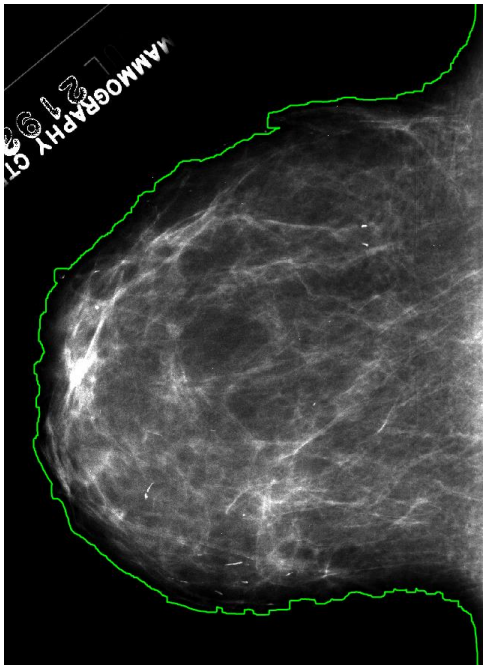

Figure 2 – Craniocaudal view of right breast

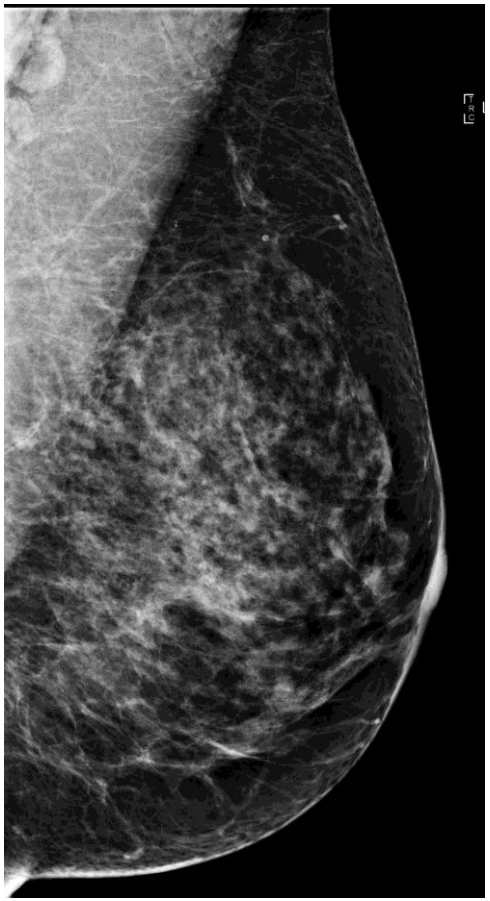

Figure 3 – MedioLateral Oblique view of left breast

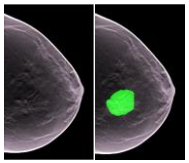

1.4 COMPUTER AIDED DIAGNOSIS

- Image Processing and Machine Learning based techniques
- Results to be reported to the doctor (not the patient)
- Aims to improve the accuracy of the whole diagnosis process

DOCTOR'S DIAGNOSIS ⟷ COMPUTER AIDED DIAGNOSIS

BI-RADS CLASSIFICATION LEVELS
BI-RADS 0
BI-RADS 1
BI-RADS 2
BI-RADS 3
BI-RADS 4
BI-RADS 5
BI-RADS 6

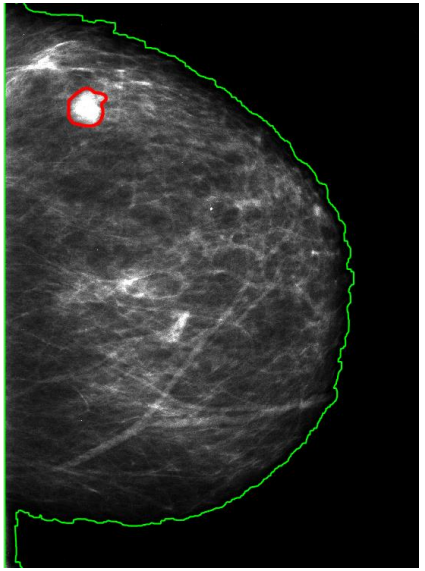

Figure 4 – Example of the application of CAD to a mammogram

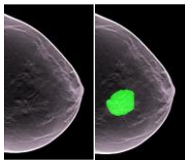

1.5 THESIS OVERALL

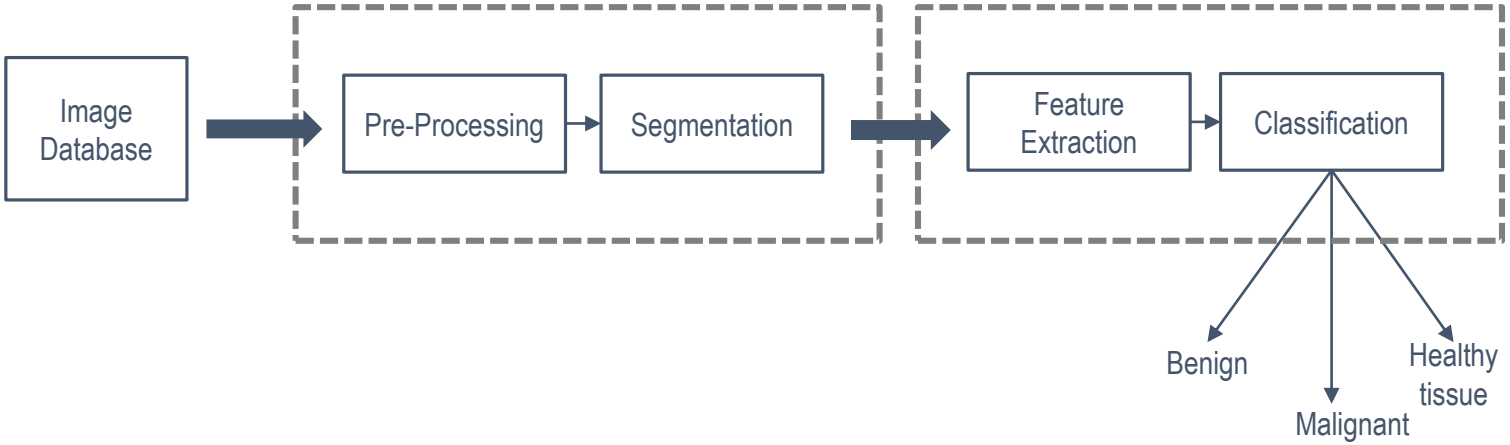

Figure 5 – Schema of the sequence of steps describing this work

PRE-PROCESSING	Bilateral Filter
SEGMENTATION	Sliding Band Filter
FEATURE EXTRACTION	Morphological, Intensity and Texture
CLASSIFICATION	Decision Tree and AdaBoost

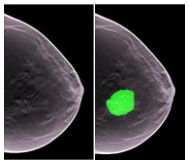

OUTLINE

- Context and Motivation
- Pre-processing and Segmentation
- Feature Extraction and Classification
- Experimental Results
- Conclusions and Future Work

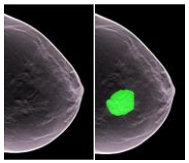

2.1 BILATERAL FILTER

- Pixel-by-Pixel technique
- Reduces Noise
- Keeps the information of the edges
- Disregards irrelevant information (including noise)
- Reduces the number of false positives

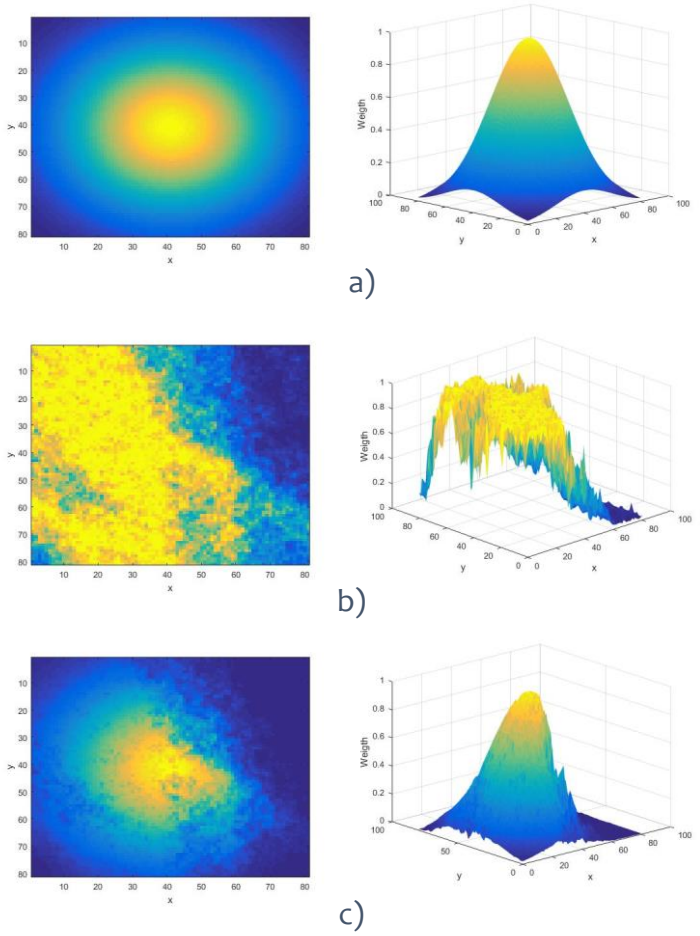

Figure 6 – 2D (on the left) and 3D (on the right) representations of a) spatial distance filter, b) intensity distance filter and c) bilateral filter.

[1] X. Qin, G. Lu, I. Sechopoulos, and B. Fei, "Breast tissue classification in digital tomosynthesis images based on global gradient minimization and texture features," in SPIE Medical Imaging. International Society for Optics and Photonics, 2014, pp. 90341V–90341V.

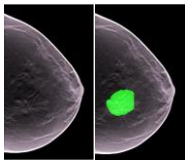

2.2 SLIDING BAND FILTER

Gradient based technique	Finds the center and the border of the ROI

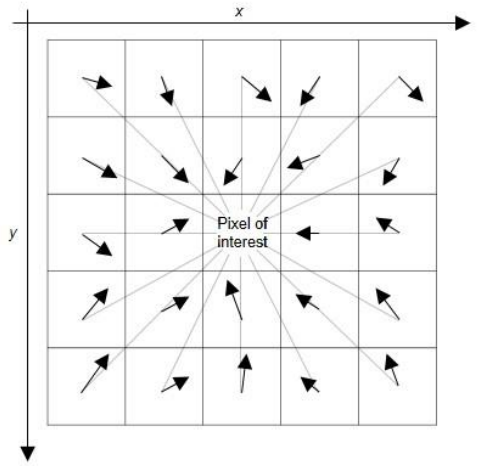

Figure 7 – Representation of the gradients of each pixel in the window of analysis of the pixel of interest -

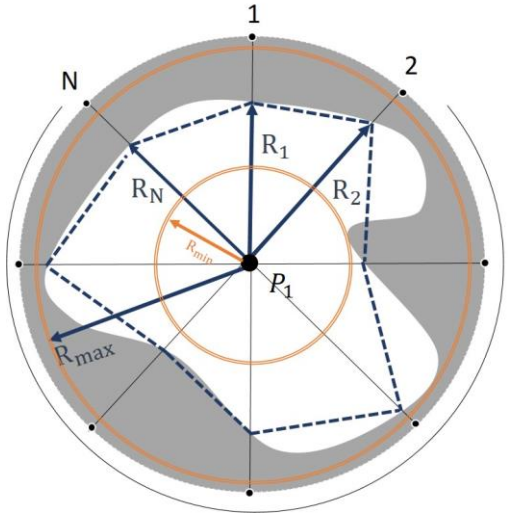

Figure 8 – Illustration of the border found by the Sliding band filter

[2] T. Esteves, P. Quelhas, A. M. Mendonça, and A. Campilho, "Gradient convergence filters and a phase congruency approach for in vivo cell nuclei detection," Machine Vision and Applications, vol. 23, no. 4, pp. 623–638, 2012.

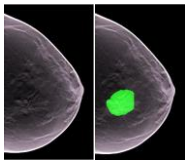

2.3 RESULTS

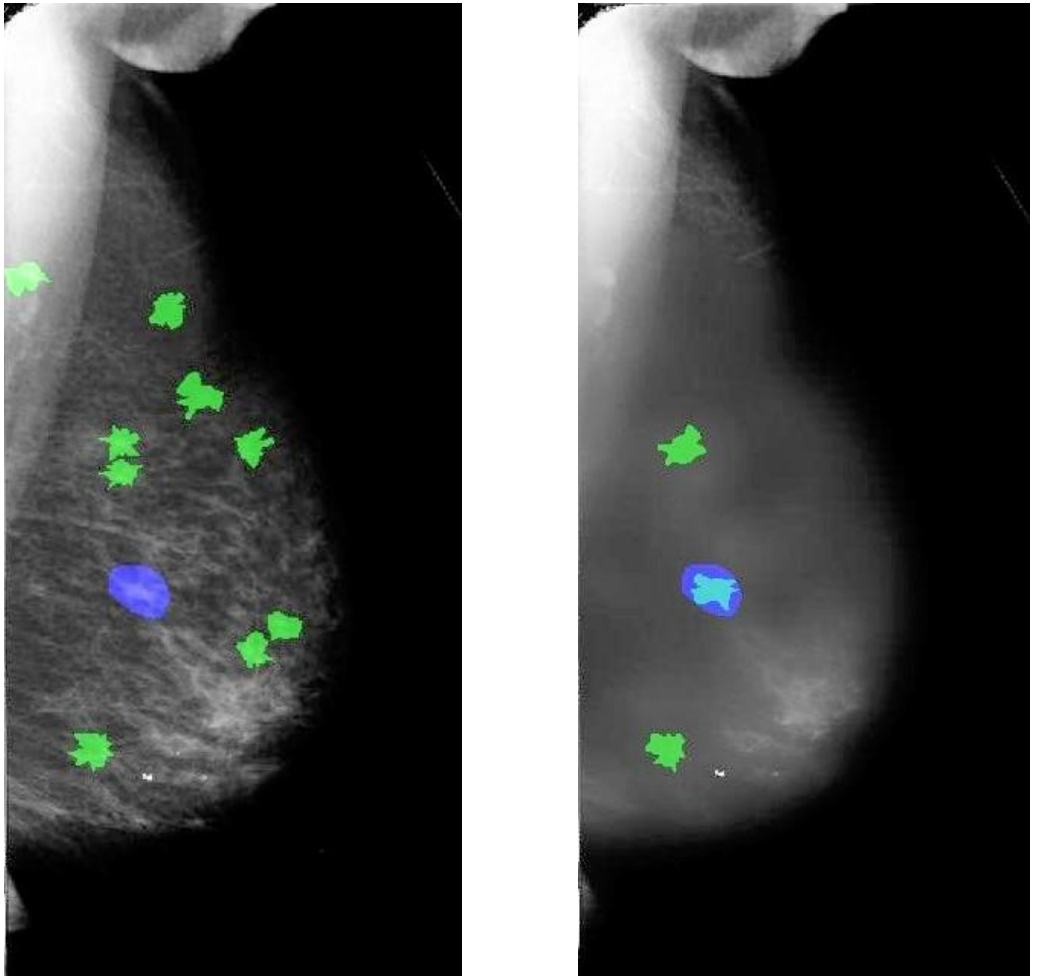

a) b)

Figure 9 – Mammogram of left breast a) not filtered and b) filtered

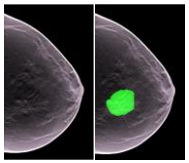

OUTLINE

- Context and Motivation
- Pre-processing and Segmentation
- Feature Extraction and Classification
- Experimental Results
- Conclusions and Future Work

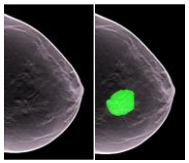

3.1 FEATURE EXTRACTION

MORPHOLOGICAL

- X and Y coordinates of the location of the centre
- Maximum Radius
- Perimeter
- Area
- Surface Change

INTENSITY

- Mean Intensity Value
- Maximum Intensity Value
- Minimum Intensity Value
- Standard Deviation of Intensity Values
- Skewness
- Kurtosis
- Contrast
- Energy
- 10 Intensity Histogram bins

TEXTURE

- Entropy
- HOG Features

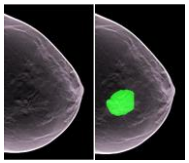

3.1 FEATURE EXTRACTION

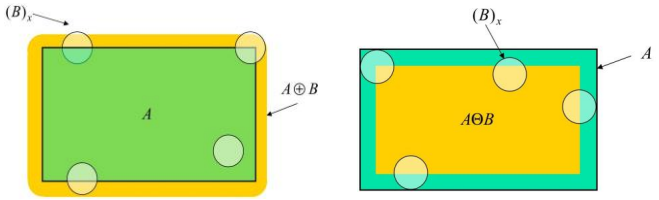

Figure 10 – Illustration of mathematical morphology operations. Dilation (on left) and Erosion (on right).

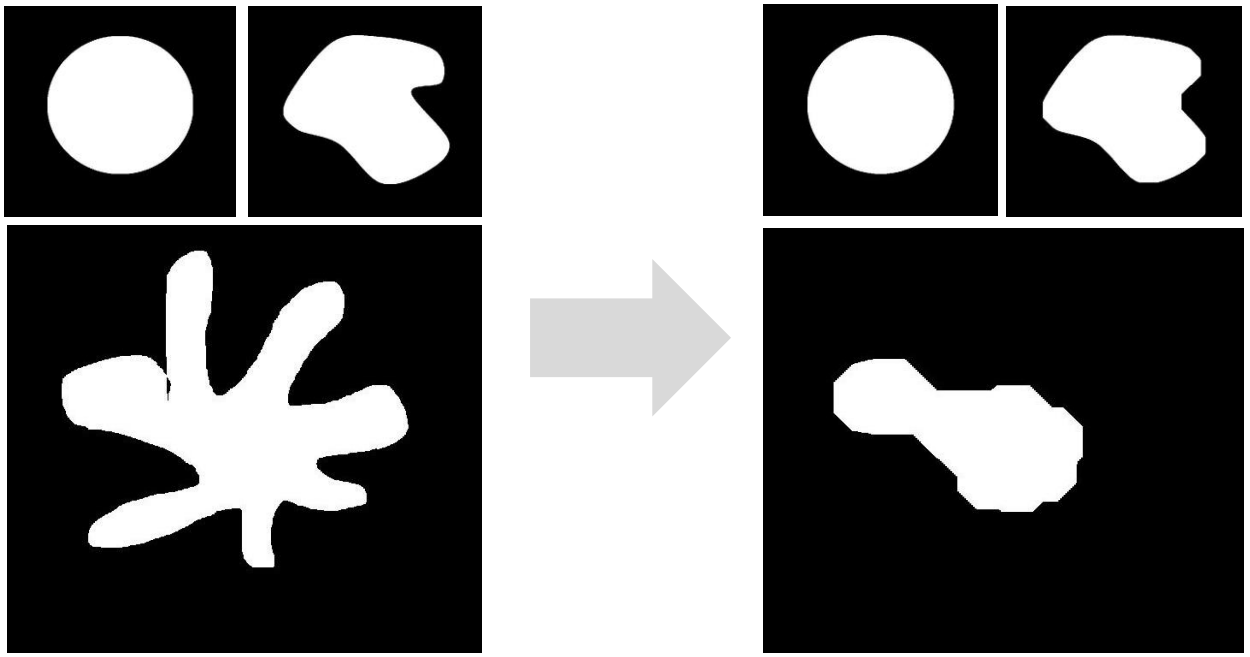

Figure 11 – Illustration of mathematical morphology opening applied to 3 different types of structures

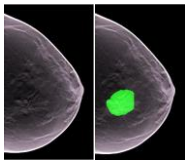

[3] Q. Zheng, "Mathematical morphology - set-theoretic representation for binary shapes," Language and Media Processing Lab - Center for Automation Research, University of Maryland College Park.

3.1 FEATURE EXTRACTION

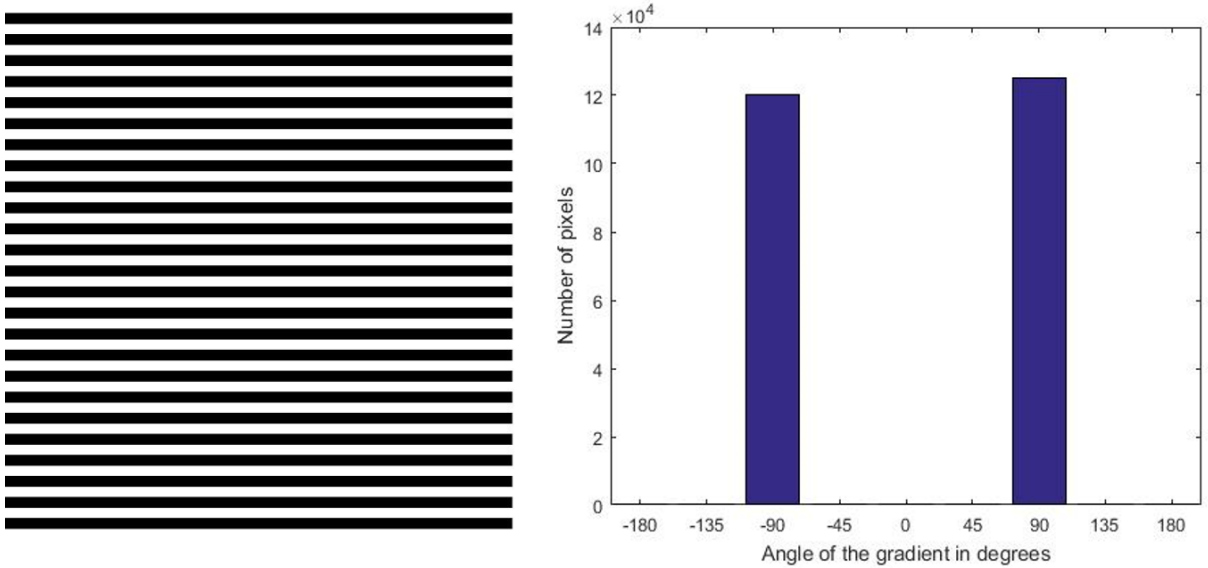

Figure 12 – Striped image (on top) and its HOG features (on the bottom).

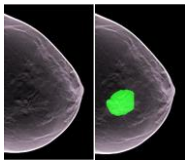

[4] M. Davis and F. Sahin, "HOG feature human detection system," in Systems, Man, and Cybernetics (SMC), 2016 IEEE International Conference on. IEEE, 2016, pp. 002878–002883.

3.2.1 SINGLE MODEL DECISION TREE

Figure 13 – Schematic representation of the classifier used in the Single Model Decision Tree experiment.

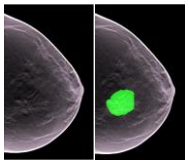

3.2.1 SINGLE MODEL DECISION TREE

- Cross Validation
- Pruned
- 100% of the dataset

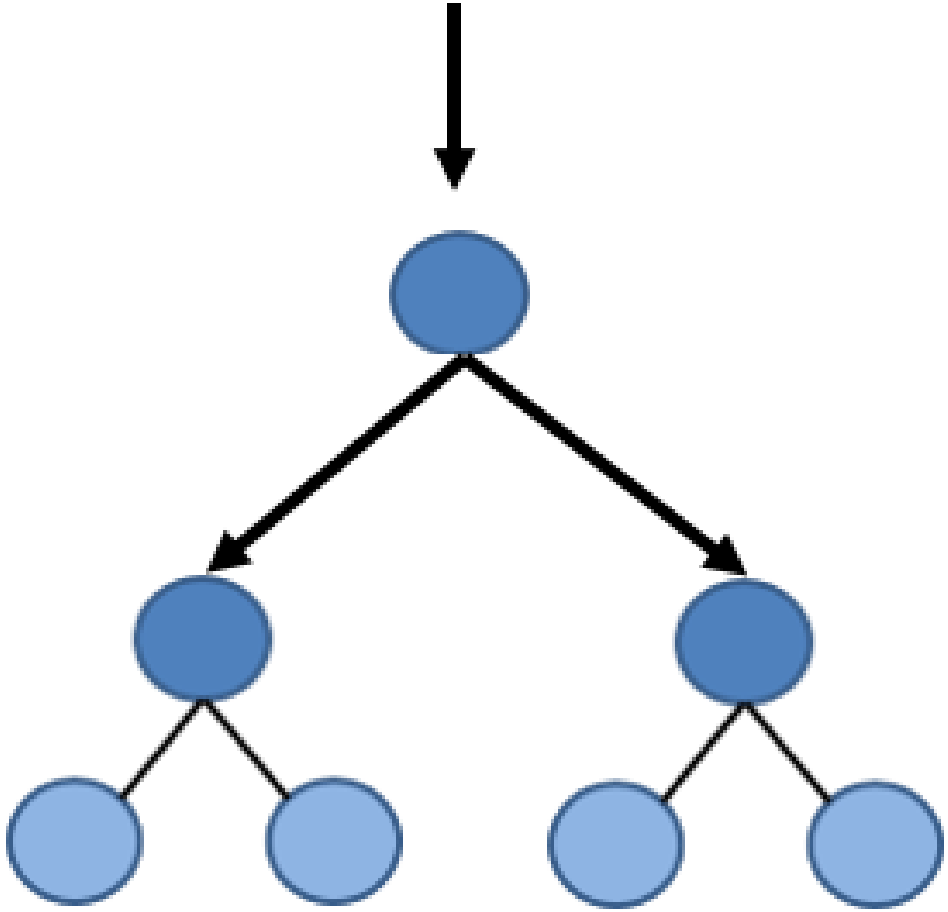

Figure 14 – Illustration of a Decision Tree.

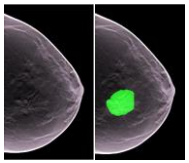

3.2.2 DECISION TREE ENSEMBLE CLASSIFIER

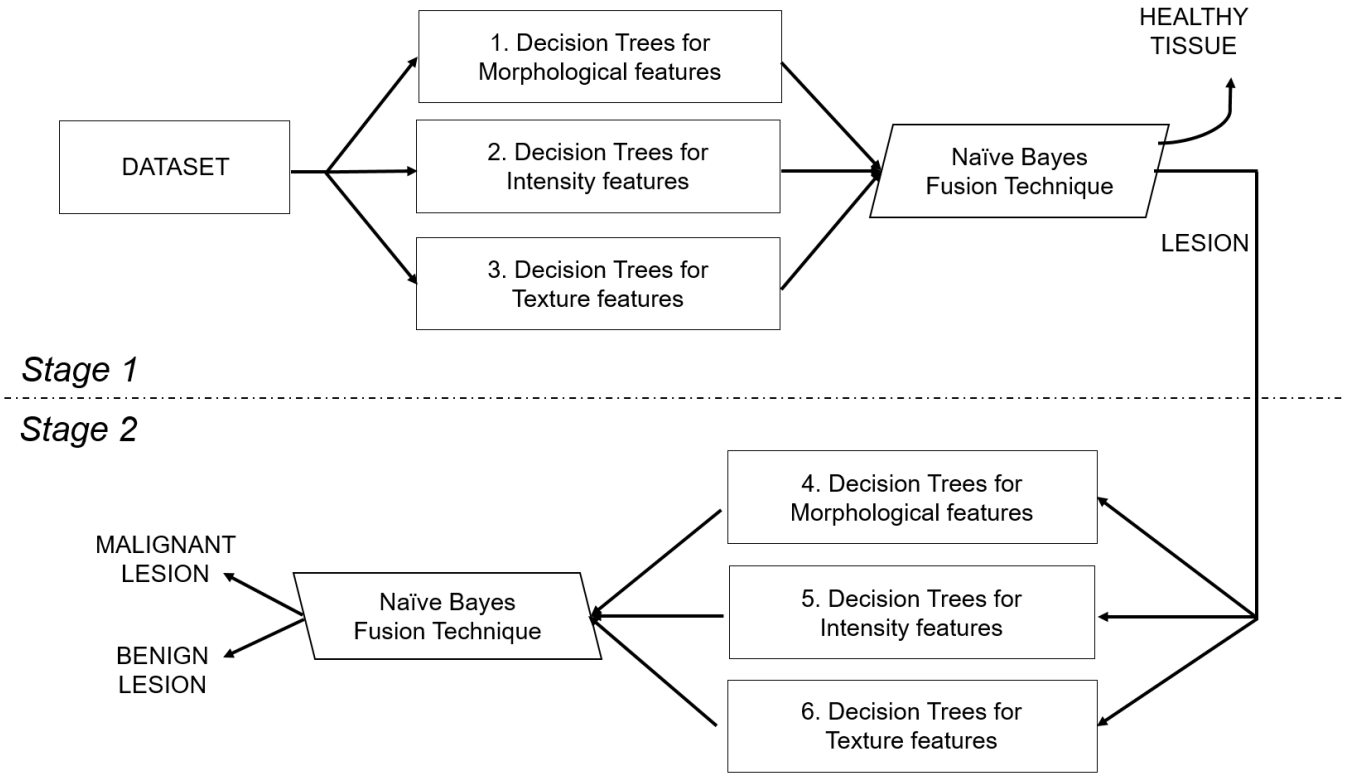

Figure 15 – Schematic representation of the classifier used in the Decision Tree Ensemble Classifier experiment.

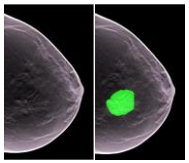

3.2.3 ADABOOST

$$h(x,f,p,\theta) = \begin{cases} 1, & if\ pf(x) < p\theta \\ 0, & otherwise \end{cases}$$

$$\epsilon^t = \min_{f,\theta,p} \sum_{i=1}^{N} w_i^{(t)} \left| h^{(t)}(x_i,f,p,\theta,p) - d_i \right|$$

$$\beta^{(t)} = \frac{\epsilon^{(t)}}{1-\epsilon^{(t)}}$$

$$w_i^{(t+1)} = w_i^{(t)} \beta^{(1-\left|h_i^{(t)} - y_i\right|)}$$

$$\alpha^{(t)} = \frac{1}{\log(\beta^{(t)})}$$

$$C(Z_i) = \begin{cases} 1, & if \sum_T \alpha^{(t)} h^{(t)}(Z_i) > \frac{1}{2} \sum_T \alpha^{(t)} \\ 0, & otherwise \end{cases}$$

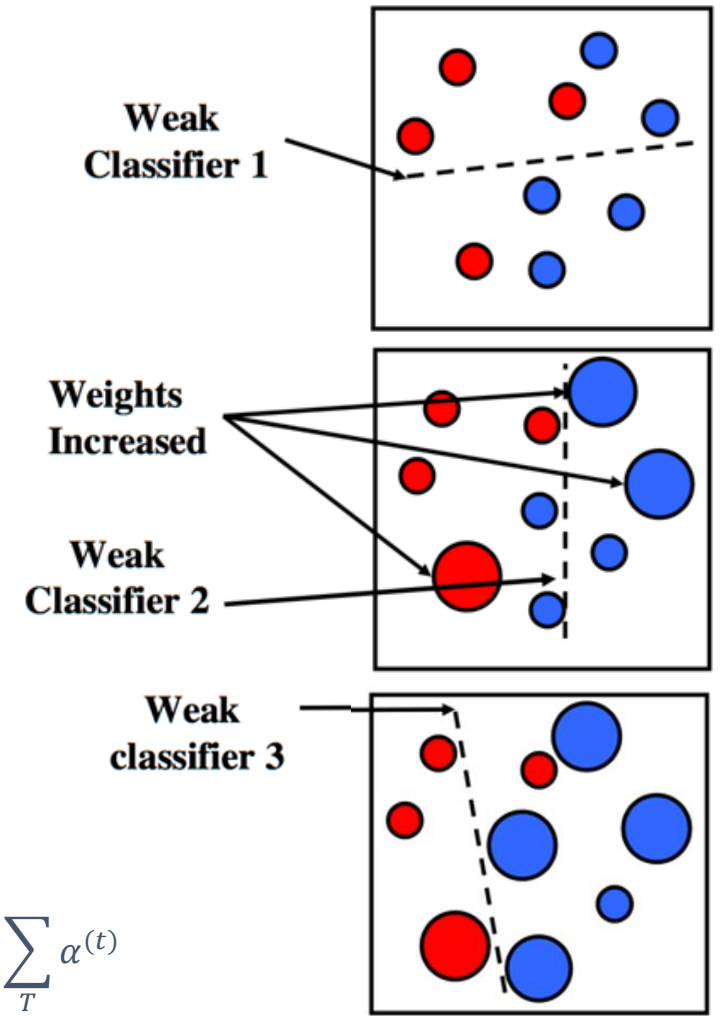

Figure 16 – Illustration of an AdaBoost Classifier.

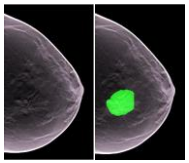

3.2.3 ADABOOST

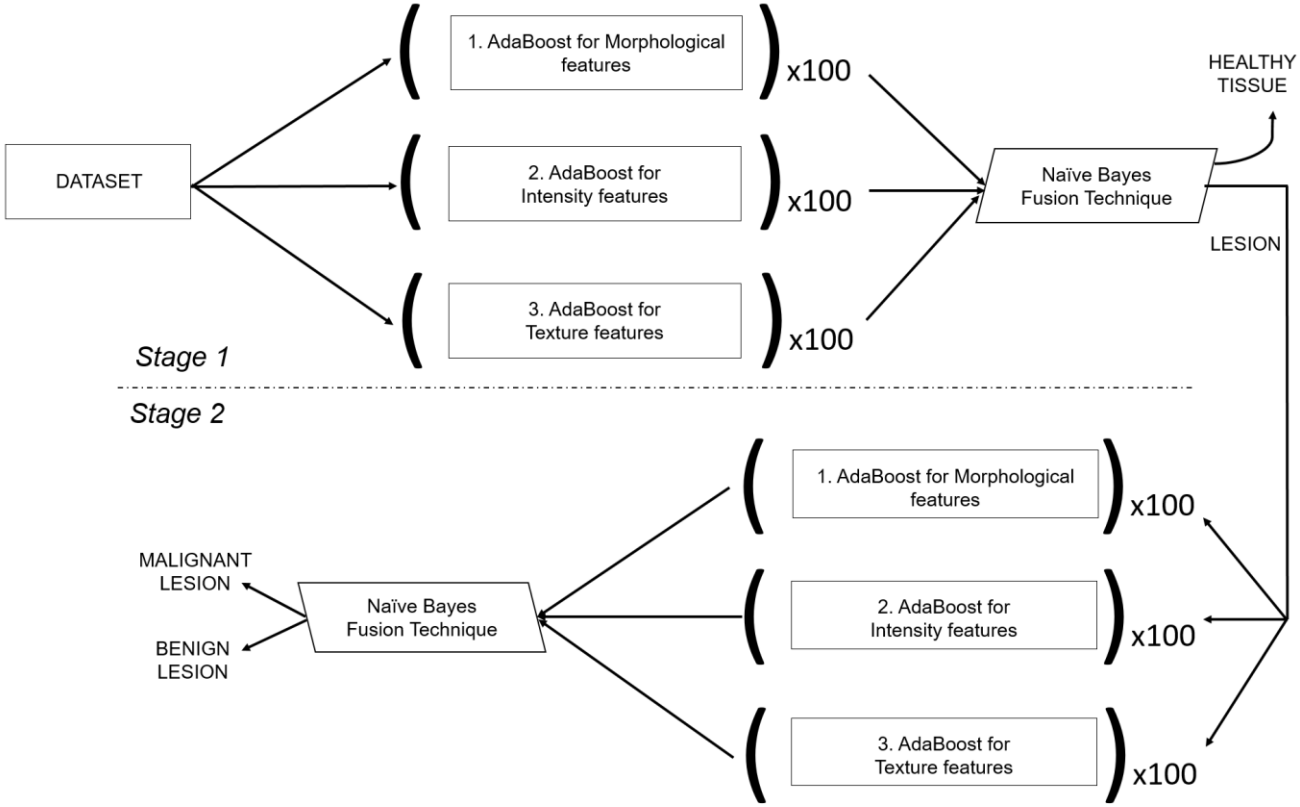

Figure 17 – Schematic representation of the classifier used in the AdaBoost experiment.

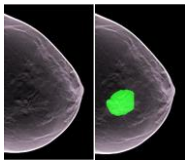

3.2.3 ADABOOST

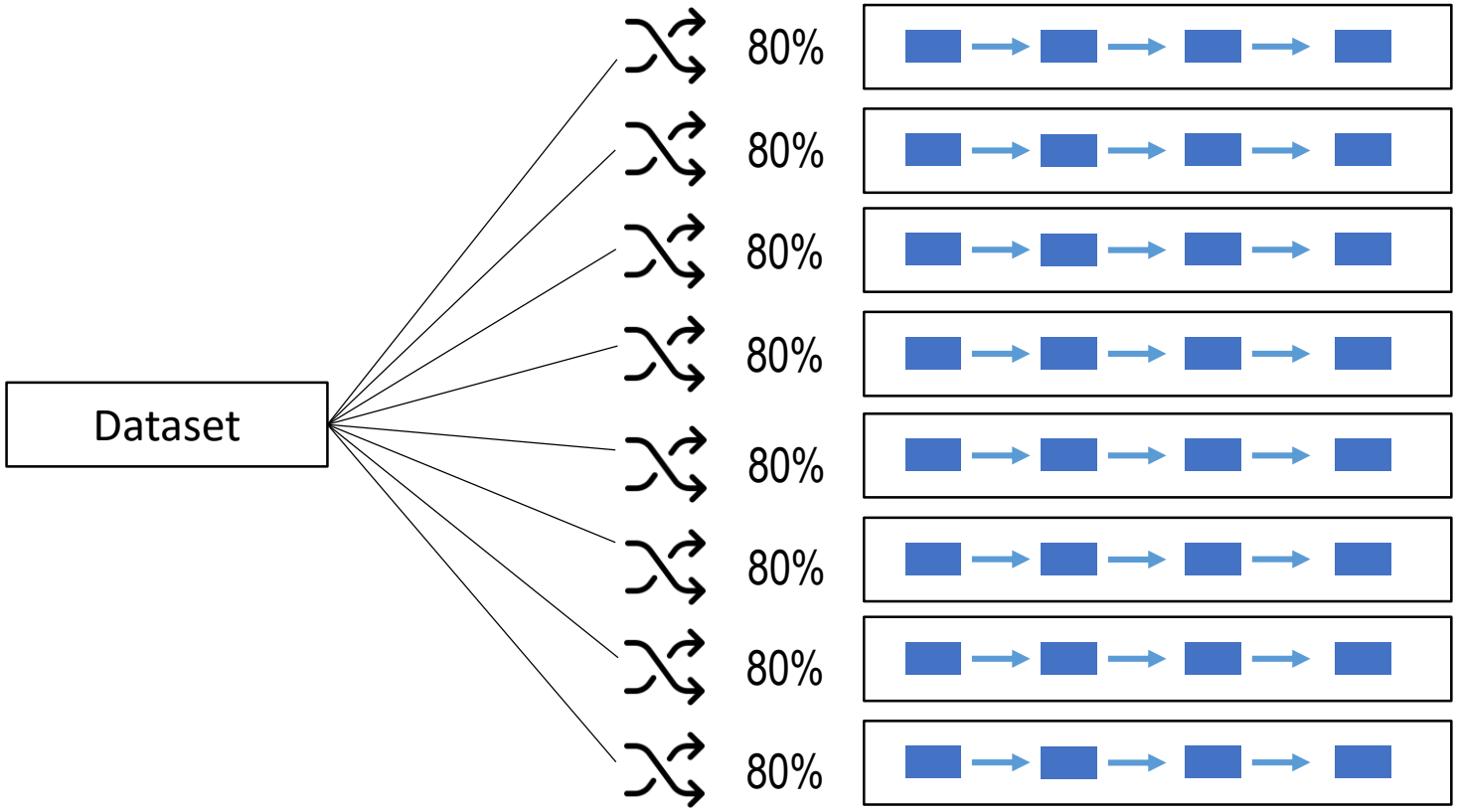

Figure 18 – Representation of bagging technique used in the AdaBoost experiment.

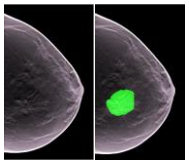

3.2.4 FUSION TECHNIQUES

NAÏVE BAYES TECHNIQUE

$$P(d_i = c \mid \boldsymbol{o}) = \frac{P(d_i = c)P(\boldsymbol{o}|d_i = c)}{P(\boldsymbol{o})} \propto \frac{1}{N_c^{K-1}} \prod_{k=1}^{K} cm_k(c, s)$$

Assume the independence between the classifiers

$$P(\boldsymbol{o}|d_i = c) = P(o_1, o_2, \dots, o_k|d_i = c) = \prod_{k=1}^{K} P(o_k|d_i = c)$$

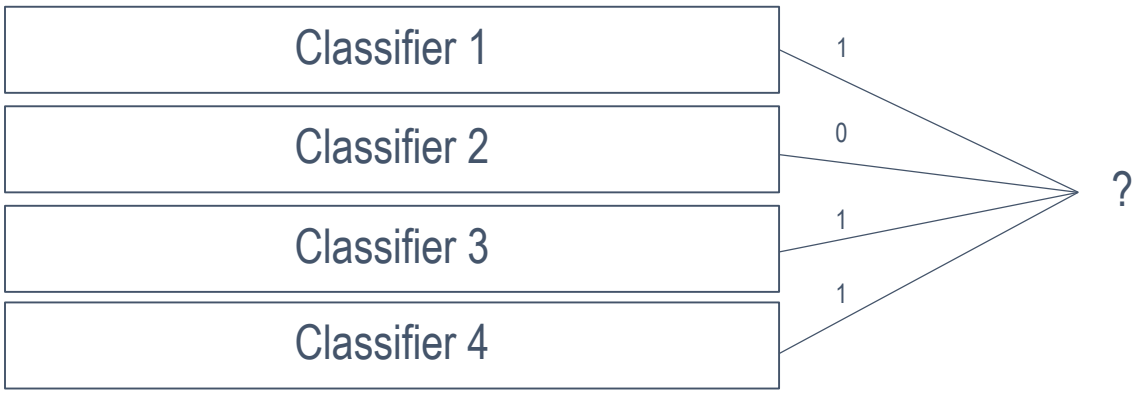

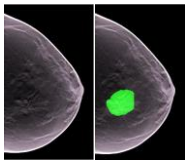

3.2.4 FUSION TECHNIQUES

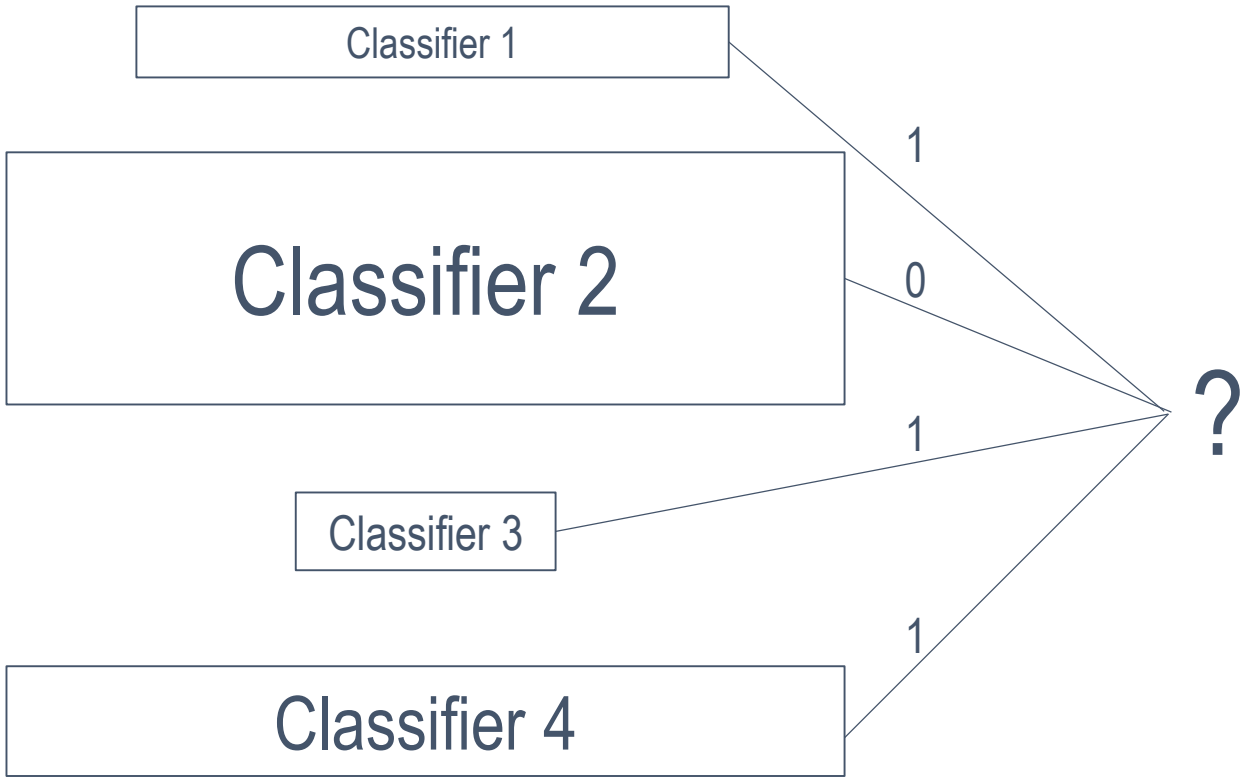

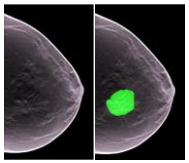

OUTLINE

- Context and Motivation
- Pre-processing and Segmentation
- Feature Extraction and Classification
- Experimental Results
- Conclusions and Future Work

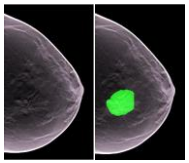

4.1 DATABASE

- 3 Experiments
  - Single Model Decision Tree
  - Decision Tree Ensemble
  - AdaBoost Ensemble
- 3185 images
  - 1950 Healthy Tissue
  - 846 Malignant Lesion
  - 399 Benign Lesions

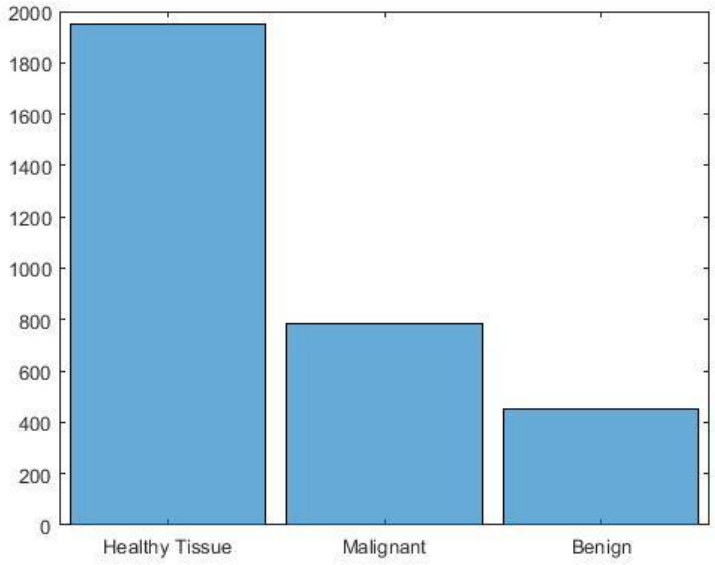

Figure 19 – Description of the database used in this work, broken down by class

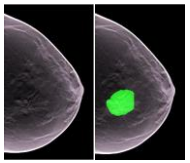

4.2 EXPERIMENTAL RESULTS

SINGLE MODEL DECISION TREE

		Output Labels		
		Healthy Tissue	Benign Mass	Malignant Mass
Target Class	Healthy Tissue	1760	83	107
	Benign Mass	136	189	125
	Malignant Mass	134	56	595

DECISION TREE ENSEMBLE CLASSIFIER

		Output Labels		
		Healthy Tissue	Benign Mass	Malignant Mass
Target Class	Healthy Tissue	1763	99	88
	Benign Mass	99	255	96
	Malignant Mass	105	80	600

ADABOOST ENSEMBLE CLASSIFIER

		Output Labels		
		Healthy Tissue	Benign Mass	Malignant Mass
Target Class	Healthy Tissue	1863	59	28
	Benign Mass	113	269	68
	Malignant Mass	81	153	551

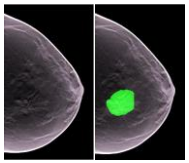

4.2 EXPERIMENTAL RESULTS

SINGLE MODEL DECISION TREE

		Output Labels		
		Healthy Tissue	Benign Mass	Malignant Mass
Target Class	Healthy Tissue	1760	83	107
	Benign Mass	136	189	125
	Malignant Mass	134	56	595

DECISION TREE ENSEMBLE CLASSIFIER

		Output Labels		
		Healthy Tissue	Benign Mass	Malignant Mass
Target Class	Healthy Tissue	1763	99	88
	Benign Mass	99	255	96
	Malignant Mass	105	80	600

ADABOOST ENSEMBLE CLASSIFIER

		Output Labels		
		Healthy Tissue	Benign Mass	Malignant Mass
Target Class	Healthy Tissue	1863	59	28
	Benign Mass	113	269	68
	Malignant Mass	81	153	551

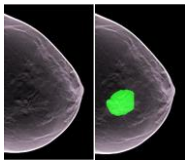

TÉCNICO LISBOA

Ciências ULisboa
Faculdade de Ciências da Universidade de Lisboa

4.2 EXPERIMENTAL RESULTS

SINGLE MODEL DECISION TREE

		Output Labels		
		Healthy Tissue	Benign Mass	Malignant Mass
Target Class	Healthy Tissue	1760	83	107
	Benign Mass	136	189	125
	Malignant Mass	134	56	595

DECISION TREE ENSEMBLE CLASSIFIER

		Output Labels		
		Healthy Tissue	Benign Mass	Malignant Mass
Target Class	Healthy Tissue	1763	99	88
	Benign Mass	99	255	96
	Malignant Mass	105	80	600

ADABOOST ENSEMBLE CLASSIFIER

		Output Labels		
		Healthy Tissue	Benign Mass	Malignant Mass
Target Class	Healthy Tissue	1863	59	28
	Benign Mass	113	269	68
	Malignant Mass	81	153	551

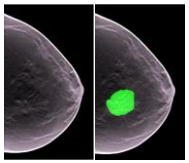

TÉCNICO LISBOA

Ciências ULisboa
Faculdade de Ciências da Universidade de Lisboa

4.2 EXPERIMENTAL RESULTS

SINGLE MODEL DECISION TREE

	Single Model Decision Tree
ACC General	0.82
ACC Malignant	0.80
ACC Benign	0.47
ACC Healthy Tissue	0.91

DECISION TREE ENSEMBLE CLASSIFIER

	Morphological Feat.	Intensity Feat	Texture Feat	Classifier ensemble
ACC General	0.80	0.73	0.71	0.82
ACC Malignant	0.62	0.42	0.43	0.77
ACC Benign	0.41	0.45	0.18	0.57
ACC Healthy Tissue	0.97	0.92	0.94	0.90

ADABOOST ENSEMBLE CLASSIFIER

	Morphological Feat.	Intensity Feat	Texture Feat	Classifier ensemble
ACC General	0.84	0.76	0.75	0.85
ACC Malignant	0.74	0.59	0.62	0.70
ACC Benign	0.46	0.27	0.20	0.60
ACC Healthy Tissue	0.97	0.94	0.92	0.96

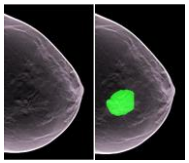

4.2 EXPERIMENTAL RESULTS

SINGLE MODEL DECISION TREE

	Single Model Decision Tree
ACC General	0.82
ACC Malignant	0.80
ACC Benign	0.47
ACC Healthy Tissue	0.91

DECISION TREE ENSEMBLE CLASSIFIER

	Morphological Feat.	Intensity Feat	Texture Feat	Classifier ensemble
ACC General	0.80	0.73	0.71	0.82
ACC Malignant	0.62	0.42	0.43	0.77
ACC Benign	0.41	0.45	0.18	0.57
ACC Healthy Tissue	0.97	0.92	0.94	0.90

ADABOOST ENSEMBLE CLASSIFIER

	Morphological Feat.	Intensity Feat	Texture Feat	Classifier ensemble
ACC General	0.84	0.76	0.75	0.85
ACC Malignant	0.74	0.59	0.62	0.70
ACC Benign	0.46	0.27	0.20	0.60
ACC Healthy Tissue	0.97	0.94	0.92	0.96

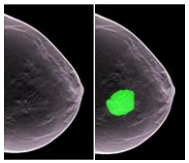

TÉCNICO LISBOA

Ciências ULisboa
Faculdade de Ciências da Universidade de Lisboa

4.2 EXPERIMENTAL RESULTS

SINGLE MODEL DECISION TREE

	Single Model Decision Tree
ACC General	0.82
ACC Malignant	0.80
ACC Benign	0.47
ACC Healthy Tissue	0.91

DECISION TREE ENSEMBLE CLASSIFIER

	Morphological Feat.	Intensity Feat	Texture Feat	Classifier ensemble
ACC General	0.80	0.73	0.71	0.82
ACC Malignant	0.62	0.42	0.43	0.77
ACC Benign	0.41	0.45	0.18	0.57
ACC Healthy Tissue	0.97	0.92	0.94	0.90

ADABOOST ENSEMBLE CLASSIFIER

	Morphological Feat.	Intensity Feat	Texture Feat	Classifier ensemble
ACC General	0.84	0.76	0.75	0.85
ACC Malignant	0.74	0.59	0.62	0.70
ACC Benign	0.46	0.27	0.20	0.60
ACC Healthy Tissue	0.97	0.94	0.92	0.96

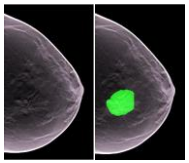

4.2 EXPERIMENTAL RESULTS

SINGLE MODEL DECISION TREE

	Single Model Decision Tree
ACC General	0.82
ACC Malignant	0.80
ACC Benign	0.47
ACC Healthy Tissue	0.91

DECISION TREE ENSEMBLE CLASSIFIER

	Morphological Feat.	Intensity Feat	Texture Feat	Classifier ensemble
ACC General	0.80	0.73	0.71	0.82
ACC Malignant	0.62	0.42	0.43	0.77
ACC Benign	0.41	0.45	0.18	0.57
ACC Healthy Tissue	0.97	0.92	0.94	0.90

ADABOOST ENSEMBLE CLASSIFIER

	Morphological Feat.	Intensity Feat	Texture Feat	Classifier ensemble
ACC General	0.84	0.76	0.75	0.85
ACC Malignant	0.74	0.59	0.62	0.70
ACC Benign	0.46	0.27	0.20	0.60
ACC Healthy Tissue	0.97	0.94	0.92	0.96

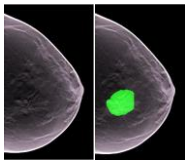

OUTLINE

- Context and Motivation
- Pre-processing and Segmentation
- Feature Extraction and Classification
- Experimental Results
- Conclusions and Future Work

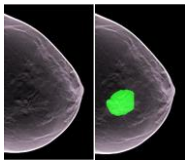

4.2 CONCLUSIONS AND FUTURE WORK

SUMMARY OF CONCLUSIONS

- AdaBoost Ensemble Classifier increases the accuracy in 3%
- Separation of the classifiers into different models improves the accuracy for benign lesions only
- Morphological Features increase a model's accuracy in 8,25%

FUTURE WORK

- Test the influence of all the parameters
- Distinguish the lesions using expert's knowledge
- Cost of classification between classes

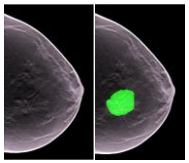

TÉCNICO LISBOA

Ciências ULisboa
Faculdade de Ciências da Universidade de Lisboa

COMPUTER AIDED DIAGNOSIS SYSTEM IN DIGITAL MAMMOGRAPHY

THANK YOU

JOÃO ROCHA E MELO

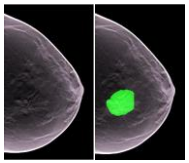

BREAST AND BREAST TUMORS

- Breast breakdown into 4 density types:
  - I, II, III, IV
- Breast Tissue divided into:
  - Adipose Tissue
  - Glandular Tissue

	Malignant	Benign
Mass	●	●
Micro Calcifications	●	●

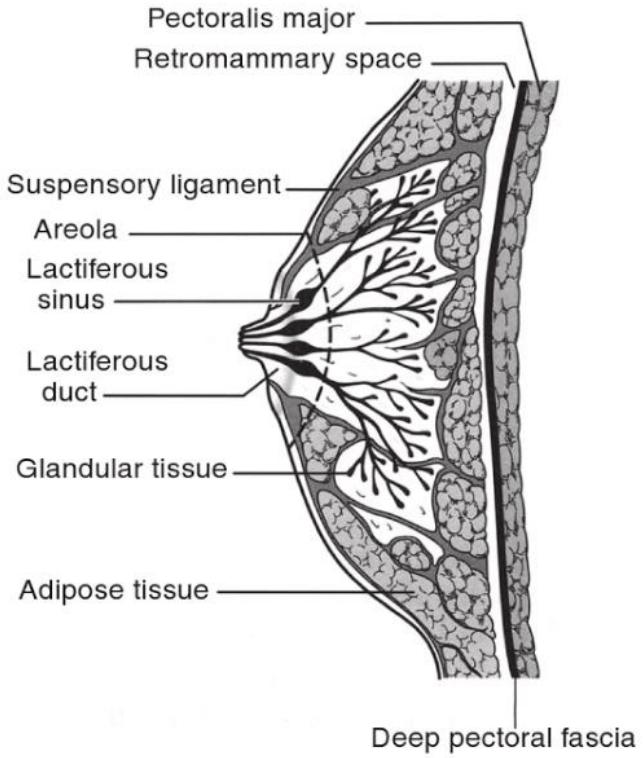

Figure 20 – Breast Illustration

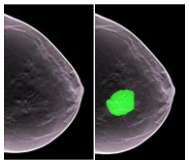

BILATERAL FILTER

- Pixel-by-Pixel technique
- Reduces Noise
- Keeps the information of the edges
- Disregards irrelevant information (including noise)
- Improves the accuracy of the segmentation stage by reducing the number of false positives

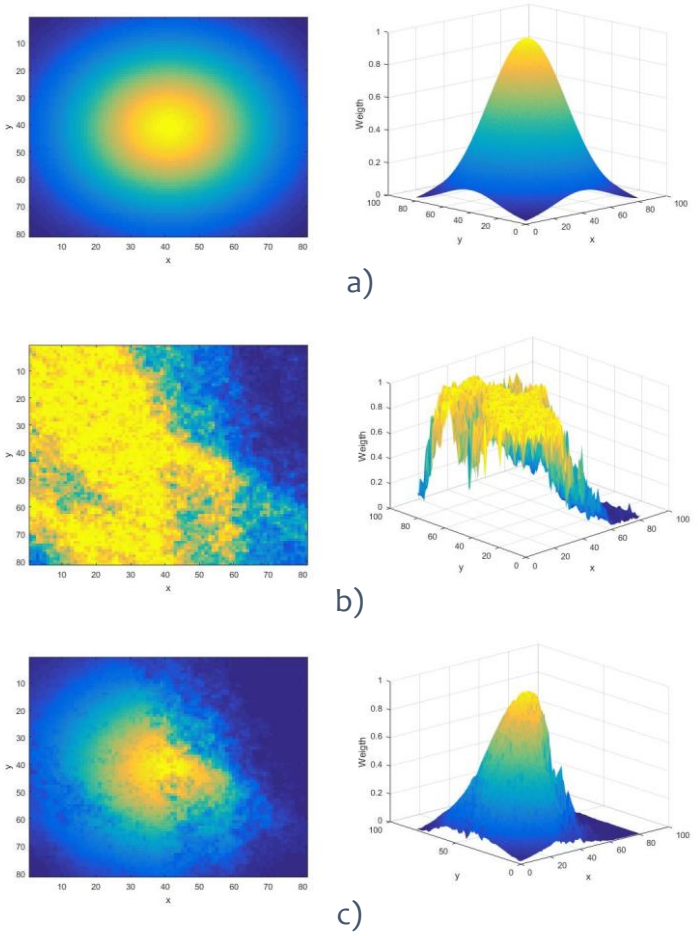

Figure 21 – 2D (on the left) and 3D (on the right) representations of a) spatial distance filter, b) intensity distance filter and c) bilateral filter

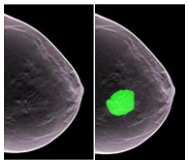

BILATERAL FILTER

Spatial Distance Filter

$$f(c_x, c_y, x, y) = \frac{e^{-|(c_x,c_y)-(x,y)|}}{\sigma_s^2}$$

Intensity Based Filter

$$g(c_x, c_y, x, y) = \frac{e^{-(I(c_x,c_y)-I(x,y))}}{\sigma_I^2}$$

Bilateral filter

$$r(c_x, c_y) = \sum_{x\ in\ \Omega} \sum_{y\ in\ \Omega} f(c_x, c_y, x, y) \times g(c_x, c_{y,}, x, y)$$

Filtered image

$$I_{BF}(c_x, c_y) = \sum_{x\ in\ \Omega} \sum_{y\ in\ \Omega} I(x, y) \times f \times g$$

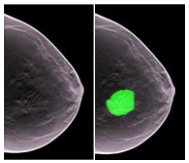

SLIDING BAND FILTER

$$DC_{SBF}(P) = \frac{1}{N}\sum_{i=1}^{N} \max_{R_{min}<R<R_{max}} \left[\frac{1}{R - R_{min}} \sum_{r=R_{min}}^{R} CI(x_i, y_i)\right]$$

Gradient based technique	Finds the center and the border of the ROI

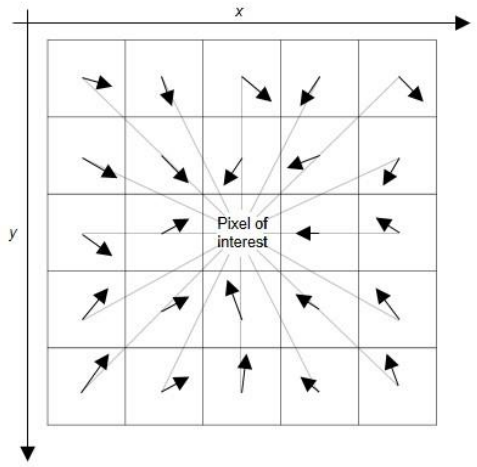

Figure 22 – Representation of the gradients of each pixel in the window of analysis of the pixel of interest -

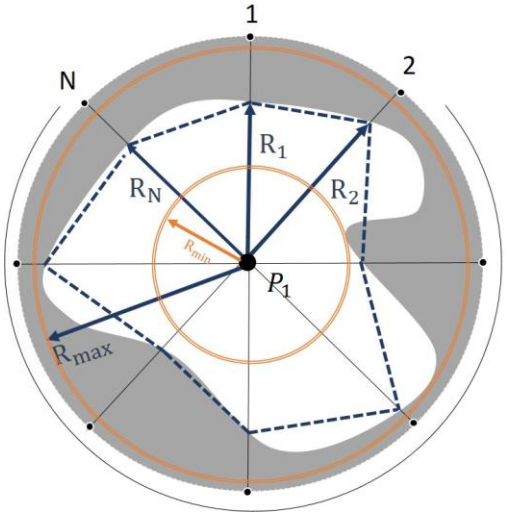

Figure 23 – Illustration of the border found by the Sliding band filter

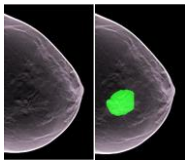

FEATURE EXTRACTION

MORPHOLOGICAL

- X and Y coordinates of the location of the centre
- Maximum Radius
- Perimeter
- Area
- Surface Change

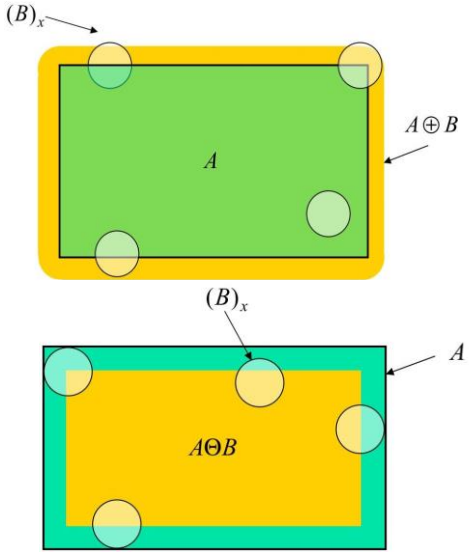

Figure 24 – Illustration of mathematical morphology operations. Dilation (on top) and Erosion (on bottom).

INTENSITY

- Mean Intensity Value
- Maximum Intensity Value
- Minimum Intensity Value
- Standard Deviation of Intensity Values
- Skewness
- Kurtosis
- Contrast
- Energy
- 10 Intensity Histogram bins

TEXTURE

- Entropy
- HOG Features

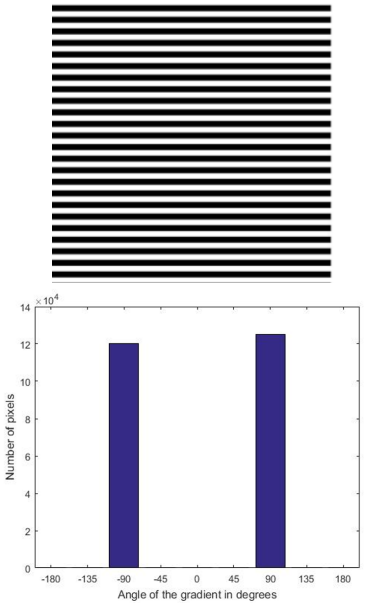

Figure 25 – Striped image (on top) and its HOG features (on the bottom).

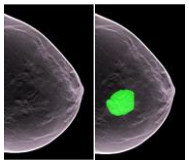

SINGLE MODEL DECISION TREE

GINI Function

$$Gini(S) = 1 - \sum_{k=1}^{C} p_s(k)^2$$

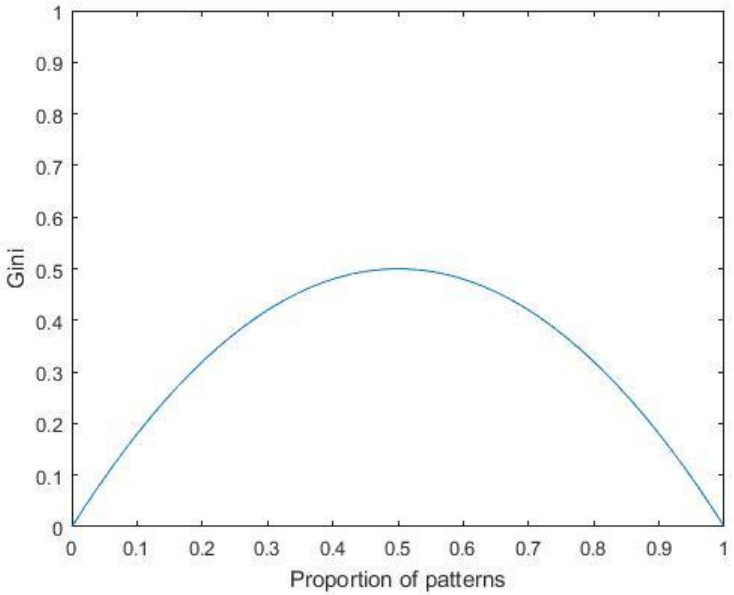

DROP

$$Drop(S, A) = Gini(S) - \sum_{v \in values(A)} \frac{|S_v|}{|S|} Gini(S_v)$$

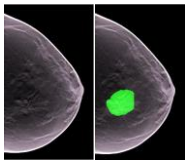

ADABOOST

$$h(x,f,p,\theta) = \begin{cases} 1, & if\ pf(x) < p\theta \\ 0, & otherwise \end{cases}$$

$$\epsilon^t = \min_{f,\theta,p} \sum_{i=1}^{N} w_i^{(t)} \left| h^{(t)}(x_i,f,p,\theta,p) - d_i \right|$$

$$\beta^{(t)} = \frac{\epsilon^{(t)}}{1-\epsilon^{(t)}}$$

$$w_i^{(t+1)} = w_i^{(t)} \beta^{(1-\left|h_i^{(t)} - y_i\right|)}$$

$$\alpha^{(t)} = \frac{1}{\log(\beta^{(t)})}$$

$$C(Z_i) = \begin{cases} 1, & if \sum_T \alpha^{(t)} h^{(t)}(Z_i) > \frac{1}{2} \sum_T \alpha^{(t)} \\ 0, & otherwise \end{cases}$$

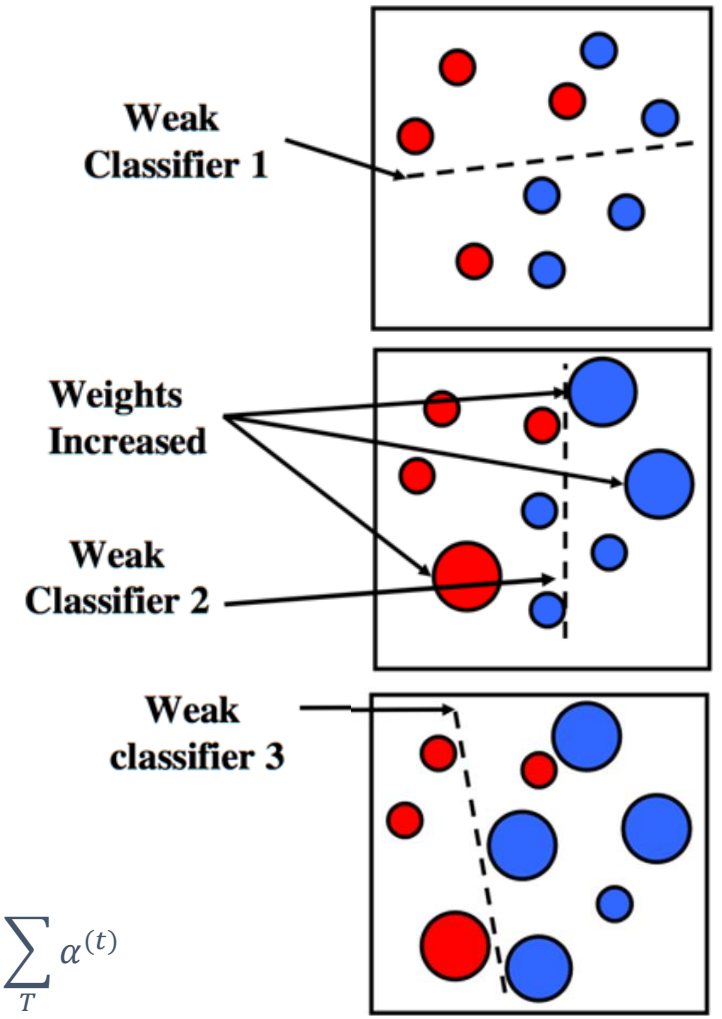

Figure 27 – Illustration of an AdaBoost Classifier

FUSION TECHNIQUES

NAÏVE BAYES TECHNIQUE

$$P(d_i = c \mid \boldsymbol{o}) = \frac{P(d_i = c)P(\boldsymbol{o}|d_i = c)}{P(\boldsymbol{o})}$$

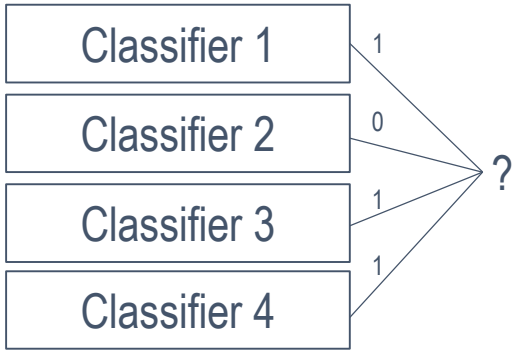

1. Disregard P(**o**)
2. $P(d_i = c) = \frac{N_c}{N}$
3. Assume the independence between the classifiers

$$P(\boldsymbol{o}|d_i = c) = P(o_1, o_2, \dots, o_k|d_i = c) = \prod_{k=1}^{K} P(o_k|d_i = c)$$

4. This can be withdrawn from:

$$P(o_k|d_i = c) = \frac{cm_k(c,s)}{N_c}$$

5. Which means that:

$$P(d_i = c|\boldsymbol{o}) \quad \propto \quad \frac{1}{N_c^{K-1}} \prod_{k=1}^{K} cm_k(c,s)$$